ACS Catalysis

pubs.acs.org/acscatalysis

Research Article

Mechanistic Understanding of the Heterogeneous, Rhodium-Cyclic (Alkyl)(Amino)Carbene-Catalyzed (Fluoro-)Arene Hydrogenation

Daniel Moock, Mario P. Wiesenfeldt,[×] Matthias Freitag,[×] Satoshi Muratsugu, Satoru Ikemoto, Robert Knitsch, Jacob Schneidewind, Wolfgang Baumann, Andreas H. Schäfer, Alexander Timmer, Mizuki Tada, Michael Ryan Hansen, and Frank Glorius*

Cite This: *ACS Catal.* 2020, 10, 6309–6317

Read Online

ACCESS | Metrics & More | Article Recommendations | Supporting Information

ABSTRACT: Recently, chemoselective methods for the hydrogenation of fluorinated, silylated, and borylated arenes have been developed providing direct access to previously unattainable, valuable products. Herein, a comprehensive study on the employed rhodium-cyclic (alkyl)(amino)carbene (CAAC) catalyst precursor is disclosed. Mechanistic experiments, kinetic studies, and surface-spectroscopic methods revealed supported rhodium(0) nanoparticles (NP) as the active catalytic species. Further studies suggest that CAAC-derived modifiers play a key role in determining the chemoselectivity of the hydrogenation of fluorinated arenes, thus offering an avenue for further tuning of the catalytic properties.

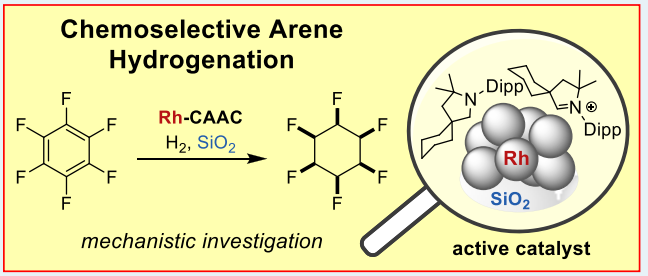

KEYWORDS: *heterogeneous catalysis, rhodium, arene hydrogenation, fluoroarenes, CAAC, nanoparticles, on-surface*

Arene hydrogenation is a powerful tool to transform readily available, planar starting materials into complex, three-dimensional building blocks.[1] These are of interest, e.g., in pharmaceutical research, and can often not be synthesized efficiently with other methods.[2] The control of the chemoselectivity, vital for the synthesis of functionalized cyclic saturated building blocks, is difficult, since very few catalysts are able to overcome the aromatic stabilization energy in absence of harsh conditions. Especially functional groups directly attached to the aromatic ring constitute a daunting challenge due to the generally prevalent hydrodefunctionalization side reaction. The bench-stable rhodium cyclic (alkyl)(amino)carbene (CAAC) precatalyst **1** in combination with a suitable additive (e.g., molecular sieves or silica gel) was essential in our recent studies on the hydrogenation of arenes bearing directly attached fluorine,[3a,b] silyl[3c] and boryl substituents,[3d] and the consecutive dearomatization-hydrogenation of fluorinated pyridines.[4] Building on research by the Bertrand group on the synthesis of CAACs[5] and their rhodium complexes,[6] this catalyst was first used by Zeng and co-workers in the preferential hydrogenation of arenes in the presence of carbonyl groups, showing a good tolerance of functional groups.[7] Although some other catalysts have proven competent in our studies, the active catalyst derived from Rh-CAAC **1** has shown a superior functional group preservation, especially for difficult substrates with fluoro, silyl, and boryl moieties.[3] Given the high synthetic utility of this precatalyst, we became interested in elucidating the catalytically active species. A general challenge in arene hydrogenation is the distinction between active homogeneous and heterogeneous species.[8] In fact, many active catalysts that were initially described as homogeneous, as they are derived from homogeneous precursors, have since been shown to actually be heterogeneous in nature.[9] The Zeng group originally assumed that the active catalyst derived from **1** is of homogeneous nature due to a mercury droplet test.[7] However, during the course of our mechanistic investigation, two studies by the Bullock group appeared providing experimental evidence for rhodium nanoparticles (NP) as active catalysts.[10] In their system, $AgBF_4$ was used to abstract chloride from **1** and initiate NP formation in the absence of another additive. Based on rhodium K-edge X-ray absorption fine structure (XAFS) analysis and IR spectroscopy (among other experiments), the authors determined that rhodium(0) NPs, which are stabilized by pyrrolidinium cation **2** (derived from the CAAC **1a** in the precursor), are the active catalyst in their case.[10a] Although Bullock and co-workers provided a thorough investigation of the active catalytic species derived from activation with $AgBF_4$, the studied conditions differ significantly from the ones found optimal in our hydrogenation methods. Most importantly, no

Received: March 4, 2020
Revised: May 4, 2020
Published: May 5, 2020

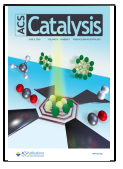

https://dx.doi.org/10.1021/acscatal.0c01074
ACS Catal. 2020, 10, 6309–6317

hydrogenation of fluorinated arenes was attempted and a silver salt was used to activate the precatalyst via a cationic pathway as opposed to molecular sieves or silica gel in our case. The resulting species derived from activation with $AgBF_4$ was evaluated by us for the hydrogenation of fluorinated arenes and proved inefficient. In fact, multifluorinated substrates such as hexafluorobenzene failed to provide any product when using an $AgBF_4$-activated precatalyst (see page S17).

Hence, a complementary study on the identity and understanding of the active catalyst system obtained in the presence of an additive like silica gel was needed. Ideally, such a study would provide a more detailed view on the chemoselective arene hydrogenation and allow for rational modifications of the catalyst in the future.

DIFFERENTIATION BETWEEN A HOMOGENEOUS AND A HETEROGENEOUS ACTIVE CATALYST

Inspired by the extensive work of the Finke group on the differentiation between heterogeneous and homogeneous active catalysts in arene hydrogenation,[8a,b,9] we began our studies with mechanistic experiments that aimed to distinguish an active heterogeneous from an active homogeneous catalyst (Figure 1). Our initial assumption of a heterogeneous reaction pathway was driven by various "telltale" signs observed during our previous studies, including the need of a stabilizing additive such as molecular sieves or silica gel, formation of a dark precipitate, and an observed induction period. In contrast to Zeng et al., we have observed a loss of catalytic activity in the presence of mercury, albeit under different reaction conditions. For the droplet test, see page S20. The conditions of the two droplet tests are adapted from the standard reaction conditions of either method, respectively, which are considerably different from one another, although both methods start with precatalyst **1**. However, the challenging reproducibility and strong dependence on reaction conditions is a known, inherent problem for mercury droplet tests and thus neither of the two possible outcomes can be used to unequivocally differentiate hetero- from homogeneous catalysis pathways and should be complemented with further experiments.[8a,b,11] Substoichiometric poisoning with tetrahydrothiophene showed the loss of catalytic activity in the reaction (see Table S3).[12] This points towards a heterogeneous active catalyst, since reactive sites would be buried inside the particles in such a system, thus requiring less than one equivalent for complete poisoning of reactivity. Furthermore, the dark gray to black solid residue obtained after hydrogenation (denoted as the residue **4**) was isolated by filtration and washed extensively with the reaction solvent. The colorless supernatant was concentrated in vacuo, and no remaining residue could be detected. The residue **4** was used as catalyst in a new reaction (Maitlis' test,[13] see Table S4) and showed fully preserved yield and selectivity, suggesting that this solid residue contained the active catalyst. Furthermore, a 3-phase-test (Collman's test)[14] was performed, in which methyl 4-hydroxybenzoate was attached to a Wang-resin and submitted to hydrogenation conditions (see page S26). No hydrogenation of the phenyl groups in the solid resin phase occurred. This is the expected outcome for a heterogeneous catalysis pathway, since a reaction is highly unlikely to occur between three phases.

We proceeded to investigate the kinetic behavior of the in situ prepared active catalyst derived from **1** and the preformed catalyst **4a** by monitoring characteristic signals of the standard substrate **5** and of the corresponding product **6** as a function of

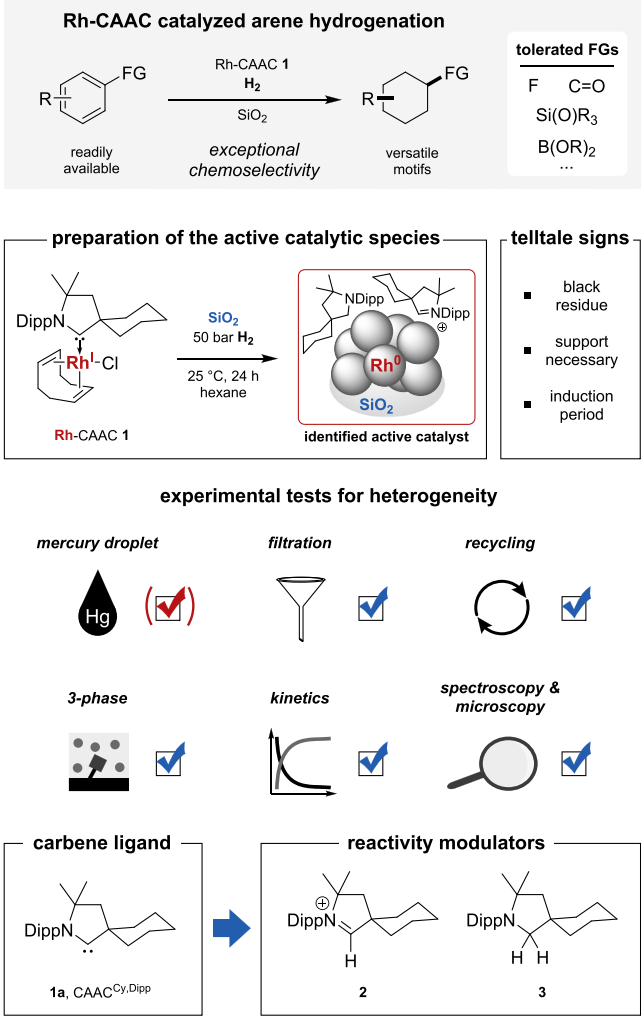

Figure 1. Overview of the established Rh-CAAC catalyzed arene hydrogenation and the studies performed in this work in order to elucidate its active catalyst species. Dipp: di*iso*propylphenyl. FG: functional group.

the reaction time using kinetic ^{1}H NMR measurements under hydrogen pressure (Figure 2). When using **1** as precatalyst in presence of silica gel, an induction period of 120−180 min was observed, which was absent when using preformed catalyst **4a**[15] (Figure 2), thus indicating that the insoluble black residue obtained after hydrogenation contains the active catalyst. In agreement with all other performed experiments, this result strongly indicates that the active catalyst is heterogeneous in nature.[16]

OBSERVATION AND CHARACTERIZATION OF NANOPARTICLES IN CATALYTIC RESIDUE 4A

The preformed catalyst **4a** was further analyzed to deeply investigate the actual structure. High-resolution transmission electron microscopy (TEM) and scanning transmission electron microscopy (STEM) with energy dispersive spectroscopy (EDS) analysis of **4a** showed the presence of rhodium NPs (Figure 3a−d). The observed lattice distances of 0.19 and 0.22 nm in the particles were attributed to a Rh(200) and Rh(111) plane, respectively. This shows that the rhodium is in metallic form (Figure 3b and page S57). The average particle size of **4a** was estimated to be 6.3 ± 2.1 nm from TEM particle

https://dx.doi.org/10.1021/acscatal.0c01074
ACS Catal. 2020, 10, 6309−6317

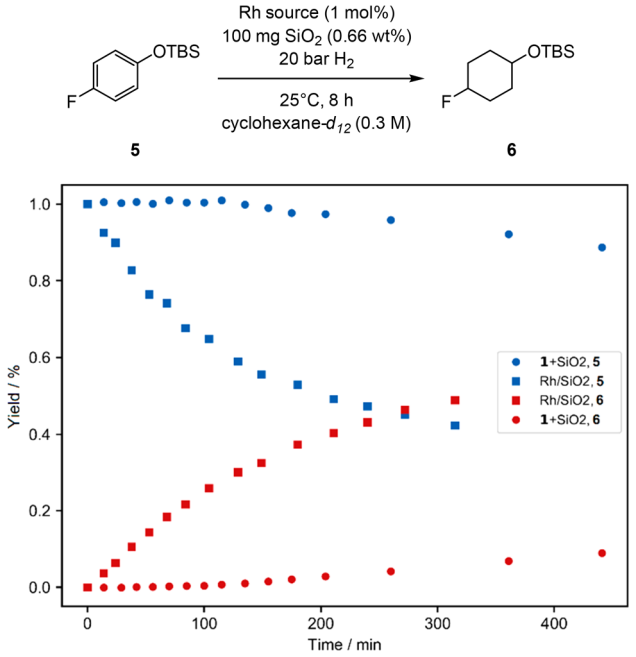

Figure 2. Yields of substrate **5** and product **6** using either precatalyst **1** + SiO_2 or preformed catalyst **4a** as a function of the reaction time. The reactions were performed in pressurized NMR tubes under hydrogen pressure and the yields were determined from the characteristic signals of **5** (proton signal at 6.77 ppm, 2H) and **6** (3.71 ppm, 1H, see pages S50–S52).

size distribution histograms (Figure 3c). X-ray diffraction (XRD) of **4a** (Figure S8) also exhibited two diffraction peaks at 41.0° and 47.4°, which were attributed to Rh(111) and Rh(200) planes of rhodium nanoparticles, respectively. The size of the rhodium NPs was also calculated by the Debye–Scherrer equation for the Rh(111) peak. The obtained value of 4.9 nm is in agreement with the TEM analysis. Rhodium K-edge X-ray absorption near edge structure (XANES, Figure 3e) indicated that the oxidation state of rhodium was close to zero. The Rh–Rh bond distance analyzed by rhodium K-edge extended X-ray fine structure (EXAFS, Figure 3f, Figure S7) was estimated to be 0.269 ± 0.003 nm (coordination number of rhodium being 8.7 ± 0.7). This is in accordance with that of rhodium metal (0.269 ± 0.001 nm), also supporting its metallic state. The Brunauer–Emmet–Teller (BET) surface area of **4a** was measured to be 398 $m^2\ g^{-1}$, which was comparable to that of the used silica gel (422 $m^2\ g^{-1}$), implying that no severe aggregation of support occurred after the formation of rhodium NPs.

PROCESS OF NANOPARTICLE FORMATION FROM RHODIUM–CAAC COMPLEX 1

In order to study the influence of the reaction time on the catalytic properties of the resulting rhodium NPs, preformed catalysts were prepared using reaction times of 3 h (**4b**) and 24 h (**4c**), respectively (Figure 4). In addition to chloride abstraction, the support is likely needed to stabilize and suppress the aggregation of growing NPs after the Rh(I) species are reduced to Rh(0).[8b] A comparison of the sizes of the formed particles with usual parameters such as the mean diameter was not possible, because the obtained size distributions were not uniform (Figure 4c). To extract information from the gathered data, we instead determined

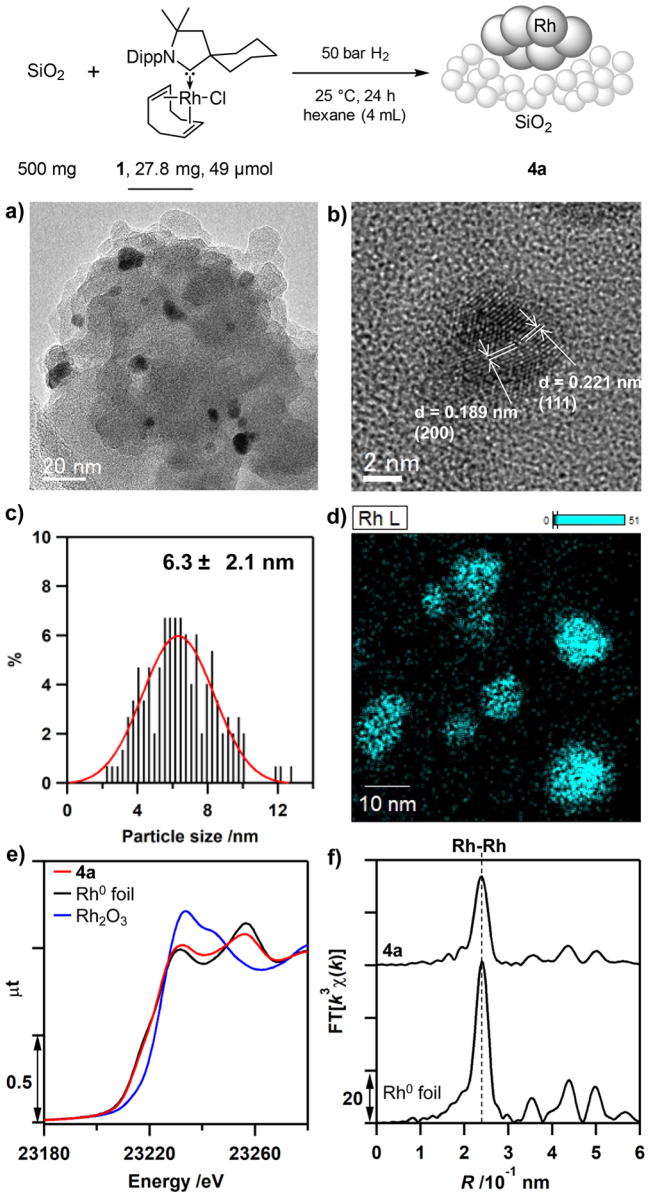

Figure 3. (a,b) TEM images of **4a** with visible lattice structure (0.19 nm Rh(200), 0.22 nm Rh(111)). (c) Histogram showing the particle size distribution of **4a**. (d) STEM-EDS image of **4a** (blue, Rh L_α characteristic X-rays). (e) Rh K-edge XANES spectra of **4a** (red), Rh(0) foil (black), and Rh_2O_3 (blue). (f) Rh K-edge EXAFS Fourier transforms of **4a** and Rh(0) foil.

the fraction of small nanoparticles, which would be the most reactive catalytic species (blue-highlighted area in Figure 4c), by defining the following parameter: $N_{s/all}$ = (number of counted particles with sizes below 3 nm)/(number of all counted particles). The fraction of the most reactive small particles was considerably larger after 3 h (**4b**, $N_{s/all}$ = 32%, Figure 4c, left) than after 24 h reaction time (**4c**, $N_{s/all}$ = 12%, Figure 4c, center). This fresh preparation of small reactive particles may explain the excellent reproducibility of our catalyst system in comparison with some commercial heterogeneous catalysts, which often show batch-dependent results for difficult reactions due to a varying particle size distribution. We also tested the influence of the amount of silica gel on the size of the rhodium NPs. Catalyst **4d**, prepared with a 3-fold excess of silica gel compared to **4b** and **4c**, and

https://dx.doi.org/10.1021/acscatal.0c01074
ACS Catal. 2020, 10, 6309–6317

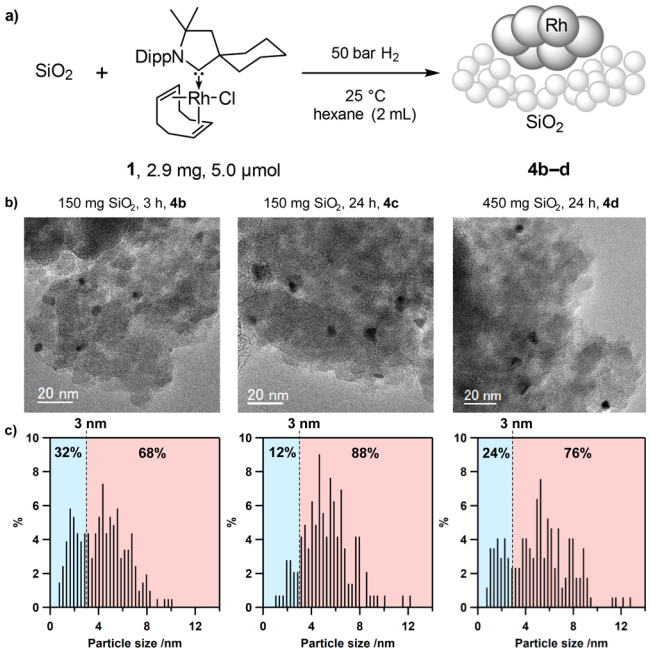

Figure 4. (a) Preparation of silica-supported NPs using different reaction times (catalysts **4b**, **4c**) or amounts of silica (catalyst **4d**). (b) Representative TEM images of **4b**–**4d**. Black dots represent areas of higher density and correspond to Rh, gray background is the silica support. (c) Histograms showing the particle size distribution of the prepared systems. Particle size distributions for all synthesized catalyst systems in this study are given in the Supporting Information.

24 h reaction time, showed a considerably increased fraction of small NPs ($N_{s/all}$ = 24%) compared to catalyst **4c** ($N_{s/all}$ = 12%). The larger number of small NPs when using more silica gel could offer one possible explanation for the observed and previously reported positive effect of increased amounts of silica gel for the hydrogenation of especially challenging highly fluorinated arenes such as hexafluorobenzene.[3d] In this previous study, increased amounts of silica led to lower amounts of defluorination and, thus, higher product yields (for a comparison see also Table S12). BET results of **4b** (395 m^2g^{-1}), **4c** (373 m^2g^{-1}), and **4d** (379 m^2g^{-1}) are very similar to those of catalytic residue **4a**. As a result, it is highly unlikely that the observed effect is caused by a surface area difference after rhodium NP formation.

LIGAND EFFECT ON CATALYSIS

We wondered if the observed high selectivity toward preservation of C–F bonds is introduced by the active ligand species derived from **1a** or if a similar selectivity could be achieved with rhodium nanoparticles of similar size and loading within the identical support material. To test this, rhodium NPs **4e**–**4g** on silica gel were prepared by impregnation of $Rh(NO_3)_3{\cdot}H_2O$ on silica gel, followed by H_2 reduction (synthesis page S6, characterization page S68; rhodium loadings were 0.87 wt % for **4e**, 5.1 wt % for **4f**, and 9.9 wt % for **4g**, respectively). No organic ligand species were attached to these rhodium NPs. When using this method, the fractions of small NPs (<3 nm) ($N_{s/all}$(**4e**) = 58%, $N_{s/all}$(**4f**) = 41%, and $N_{s/all}$(**4g**) = 27%) were somewhat higher than those obtained when using catalysts derived from Rh–CAAC **1** as precursor (e.g., **4a**–**d**). It is worth noting that we observed that an increased fraction of small NPs affects higher yields and that the fraction of small NPs decreases with an increased amount of rhodium down to 27%, which is less than that observed for catalyst **4b**. The average particle size of **4e** was estimated to be 2.8 ± 0.7 nm determined from particle size distribution histograms (Figure S12), which is slightly smaller than that of **4a** with similar Rh loading. When the rhodium loading was increased, average particle sizes were slightly increased (3.2 ± 0.8 nm for **4f** and 3.5 ± 1.0 nm for **4g**, respectively).

Catalytic reaction results for the hydrogenation of the model substrate **5** are summarized in Table 1 (see also Table S11).

Table 1. Comparison of Catalytic Performance of Different Rh/SiO_2 Systems for the Hydrogenation of 5[a]

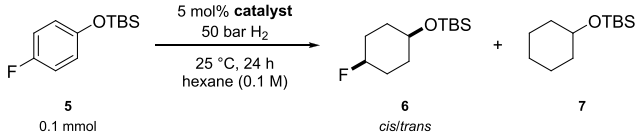

catalyst	Rh amount [wt %]	yield of **6** [%] (d. r.)	yield of **7** [%]
Rh–CAAC **1**/SiO_2	1.0	90 (94:6)	3
Rh–CAAC **1**/SiO_2	5.1	86 (94:6)	4
Rh/SiO_2 **4a**	1.0	89 (94:6)	3
Rh/SiO_2 **4e**	0.87	66 (87:13)	18
Rh/SiO_2 **4f**	5.1	59 (89:11)	23
Rh/SiO_2 **4g**	9.9	68 (88:12)	23

[a]Yields were determined via GC-FID against mesitylene as internal standard. Numbers do not add up to unity, because cyclohexane and cyclohexanol are formed as byproducts, which coelute with the solvent and thus cannot be detected.

4e–**4g** all showed a significantly increased amount of defluorination when compared to the standard system (precursor **1** used, in situ generation of **4**). In addition, the *cis*-selectivity of the NP systems is decreased. Therefore, the selectivity of the investigated system cannot be solely dependent on the NP size or rhodium loading.

OBSERVATION AND IDENTITY OF LIGAND SPECIES ON THE CATALYST SURFACE

The comparison of the catalytic results obtained using **4a** and **4e**–**4g** suggested that catalyst performance is influenced by a ligand species. Therefore, we proceeded to characterize catalyst **4a** and investigate if ligand species were present on the surface of the NPs. X-ray photoelectron spectroscopy (XPS) of catalyst **4a** revealed a broad nitrogen signal at 400–402 eV (Figure 5). The best fitting to the given data is obtained with two signals in a 1:1 ratio, separated by more than 2 eV. While the intensity of the nitrogen signal (as well as that of the rhodium signal) is low due to the sparse dispersion within the silica, the significant distance between the fitted signals strongly suggests the existence of two different nitrogen species. Given that the CAAC ligand **1a** is the sole nitrogen containing species in the precursor, two different nitrogen-containing species must have formed from that ligand under the reaction conditions. To elucidate the identity of the two unknown nitrogen-containing species in the sample, we turned to solid-state NMR spectroscopy. To overcome the problem of the sparse density of possible residues, complex **1** was prepared with a ^{13}C-enriched CAAC precursor. The synthesis of the labeled CAAC precursor was conducted starting from commercially available isotope-labeled benzoic acid, using

https://dx.doi.org/10.1021/acscatal.0c01074
ACS Catal. 2020, 10, 6309–6317

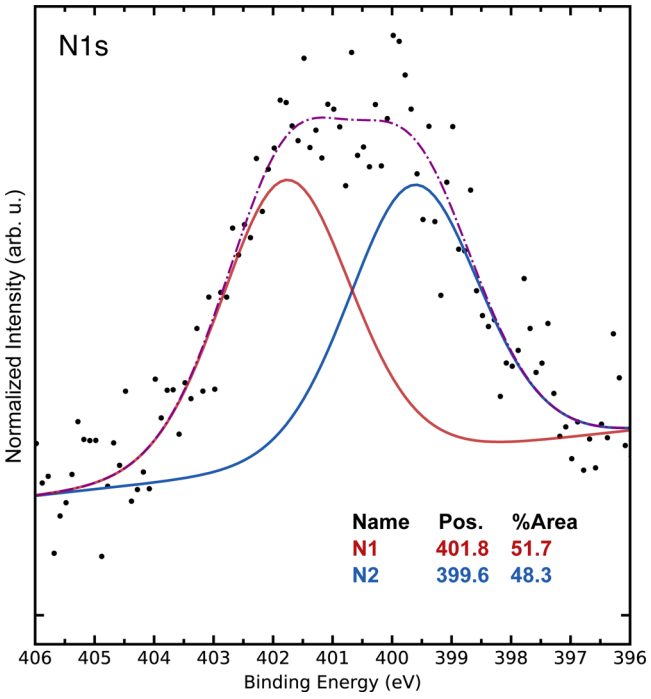

Figure 5. Plotted signal and fitting of the nitrogen-containing species, determined by XPS.

our own protocol for arene hydrogenation (see page S9 for the full synthetic route).[3e,17]

Samples for $^{13}C\{^{1}H\}$ CP/MAS NMR spectroscopy were prepared by stirring the labeled complex with silica gel under hydrogen atmosphere (cf. Figure 4a).[18] The obtained $^{13}C\{^{1}H\}$ CP/MAS NMR spectrum shows two intense ^{13}C signals at ~186 and ~65 ppm (Figure 6). Comparison with the spectrum of the labeled complex **1** confirmed that the signal at 186 ppm cannot be assigned to a ligated carbene species. Given our extensive experience in the field of carbenes on surfaces and given the high strength of carbene−metal bonds, this result was unexpected at first.[19] However, the excellent overlap with the labeled signal of the ^{13}C-enriched pyrrolidinium salt **2** suggested that this iminium cation is likely one of the two nitrogen-containing species.

That cation is likely generated by a reductive elimination of carbene and hydrogen from an intermediate carbene metal−hydride complex, as previously proposed by the Ananikov group.[20] An alternative pathway could be the dissociation of the carbene ligand and subsequent protonation by acidic silanol groups present within the silica gel. However, a dissociation of a free carbene is unlikely regarding the strength of carbene−metal bonds. Chloride is most likely the counteranion, although deprotonated silanol groups are also imaginable. Given that the iminium moiety present in **2** is reducible under hydrogenation conditions, we assumed that the remaining species corresponding to the ^{13}C signal at ~65 ppm might be the amine **3**. Hence, pyrrolidine **3** was synthesized from pyrrolidinium **2** (with chloride as a counteranion) by reduction with $LiAlH_4$. In agreement with our assumption, pyrrolidine **3** showed a distinct signal at 64.9 ppm in deuterated chloroform. It is worth noting that amines are known ligands for nanoparticles.[21] Comparison of spectra of labeled and unlabeled pyrrolidinium **2** further suggests that the smaller signals between 5 and 0 ppm are

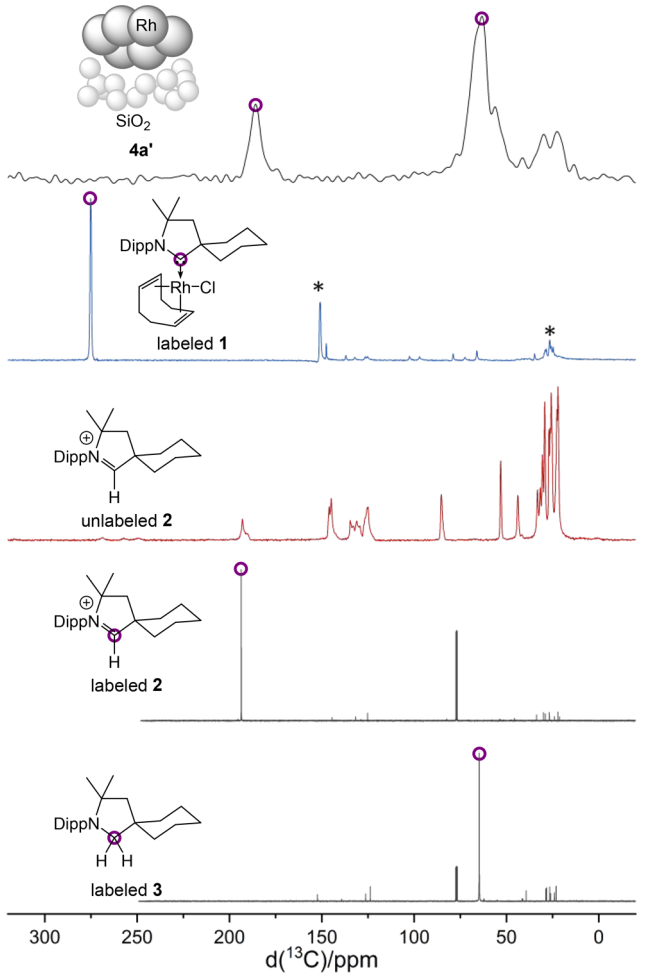

Figure 6. $^{13}C\{^{1}H\}$ CP/MAS NMR spectra of **4a′** prepared from the ^{13}C-labeled complex **1** (black), labeled complex **1** (blue), and unlabeled **2** (red). Peaks corresponding to the labeled carbon are highlighted. The two bottom spectra allow for a comparison with to the pure, ^{13}C-labeled compounds **2** and **3** in solution. *Spinning side bands of the main signal.

derived from the backbone of the pyrrolidinium cation and the pyrrolidine.

BOTTOM-UP SYNTHESIS OF A RELATED SELECTIVE HYDROGENATION CATALYST

Given the previous finding that the observed high chemoselectivity of the hydrogenation of fluorinated arenes is not solely determined by the particle size of the used rhodium catalyst, we wondered if the species **2** and **3** may have an influence on the catalytic activity and selectivity. In previous studies on the influence of ligands such as phosphines and phosphites on reactions catalyzed by Rh NPs, significant effects on the reactivity and selectivity of hydrogenation reactions were observed.[22a−c]

Furthermore, imidazolium based ionic liquids, which were covalently anchored to the Al_2O_3-support, were shown to influence the catalytic hydrogenation of benzene with dispersed Ru NPs.[22d] Driven by these reports, we set out to prepare a catalyst system similar to **4a** by adding **2** and **3** to synthesized rhodium NPs on silica (**4e−4g**) and to commercial rhodium on alumina (Table S9). These were tested for the hydrogenation of model substrate **5** using a

https://dx.doi.org/10.1021/acscatal.0c01074
ACS Catal. 2020, 10, 6309−6317

catalyst loading of 1 mol %. We started by investigating the optimal ratio of both additives at a combined loading of 1.0 equivalents relative to the used rhodium but no clear trend emerged (see Table S11). The use of one equivalent of a single species only led to high amounts of defluorination (for pyrrolidine **3**) or incomplete conversion (for pyrrolidinium **2**). These results strongly suggest that both species **2** and **3** seem to play an important role in modifying the catalytic activity. For further experiments, we therefore kept a 1:1-ratio of these species, as suggested by the XPS studies. Next, varying equivalents of that 1:1 mixture with regard to rhodium were investigated (Figure 7). The studies showed an increase in

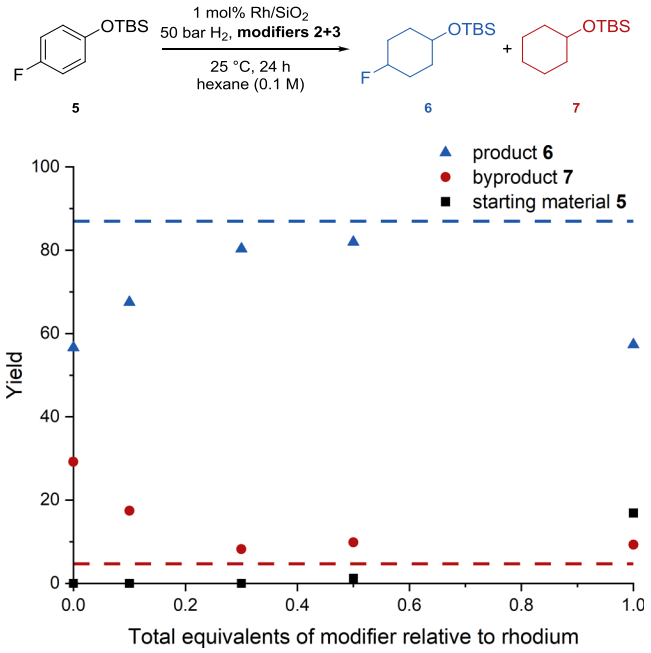

Figure 7. Yields of product **6** and byproduct **7** obtained by the hydrogenation of substrate **5** with Rh NPs on silica gel **4e** as a function of the total equivalents of a 1:1 mixture of pyrroldinium **2** and pyrrolidine **3**, which were added to the Rh NPs. Yields were determined by GC-FID analysis vs mesitylene.

conversion with decreased amounts of the modifiers. Full conversion was still achieved with as little as 0.3 equiv of the modifier mixture. Further decreasing the amount of the modifiers resulted in a significant increase in defluorination. The amount of defluorination and the obtained yield with 0.3 equivalents of a 1:1 modifier mixture was almost identical to the values observed when using the precursor **1** with silica gel and in situ generation of the active catalytic system (**4**).

As additional control experiments, preformed rhodium particles, obtained by submitting Rh(COD)Cl and silica gel to hydrogenation conditions, were tested untreated and treated with the modifiers **2** and **3**. While reactivity was observed for the former case, a complete loss of activity was noted with one equivalent of the modifier mixture, irrespective of their ratio (see Table S10). We wondered whether the identity of the rhodium ligand, in this case CAAC **1a**, may also influence the NP formation. To investigate this, different CAAC ligands **8** and **9** were used during the preparation of rhodium particles **4h** and **4i**, respectively (Figure 8). As expected, the size distribution of those rhodium particles differed from that of the active catalyst **4a** derived from ligand **1a** in the precursor

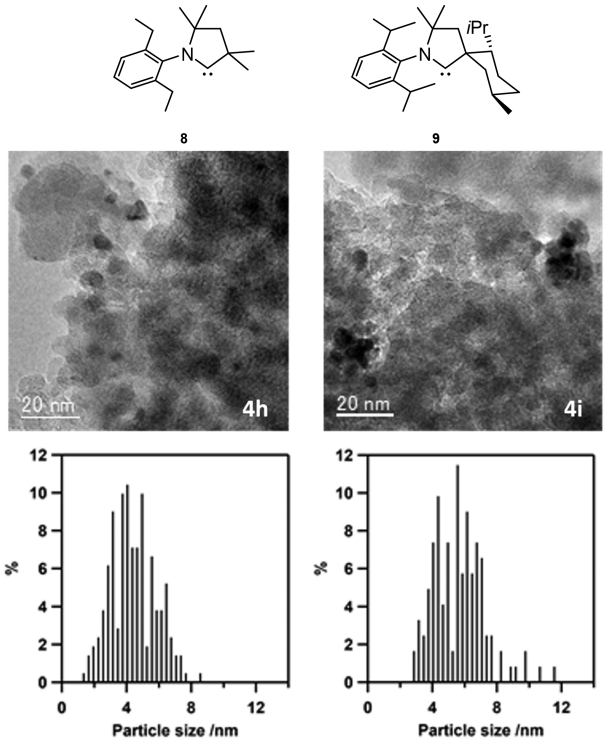

Figure 8. Structures of alternative CAAC ligands **8** and **9** with representative TEM images of corresponding rhodium particles obtained from complex precursors and the size distribution.

complex. More importantly, the catalytic results differed significantly as well (see Figure S1, Table S6) with the residues **4h** and **4i** showing either strongly reduced or no activity at all (see page S29 for a more detailed discussion).

The preformed catalyst **4e** (with and without modifiers) was also investigated for the hydrogenation of hexafluorobenzene **10**, since for this substrate the difference in chemoselectivity compared to other catalysts was especially pronounced. When applying the determined optimized amounts of modifiers to the preformed NPs the yield for hexafluorocyclohexane **11** could be increased from 4% (no modifiers) to 29% with modifiers. This constitutes 74% of the yield obtained with the established precursor Rh−CAAC **1** under otherwise identical conditions (Table 2).

In conclusion, we have elucidated the active catalyst derived from a molecular Rh−CAAC precursor, which has previously

Table 2. Comparing the Performance of Synthesized and Modified NPs with the Standard Catalyst System[23,a]

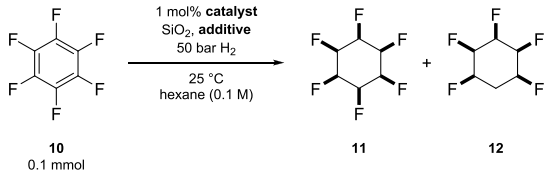

catalyst	yield **11** [%]	yield **12** [%]
Rh−CAAC **1**/44 mg SiO_2	39	22
Rh/SiO_2 (**4e**, 0.87 wt %) with 0.3 equiv of **2** and **3** (1:1)	29	8
Rh/SiO_2 (**4e**, 0.87 wt %)	4	57

[a]Isolated yields are given.

https://dx.doi.org/10.1021/acscatal.0c01074
ACS Catal. 2020, 10, 6309−6317

been shown to enable a highly chemoselective hydrogenation of a broad scope of (fluorinated) arenes and heteroarenes. By combining mechanistic and kinetic studies, we confirmed that the active catalyst is heterogeneous in nature. Various imaging, spectroscopic, and surface analysis techniques revealed silica gel-supported rhodium(0) NPs as active catalytic species. After excluding the presence of a metal-bound carbene species on the NPs, we further determined that CAAC-derived pyrrolidinium **2** and pyrrolidine **3** act as modifiers that are key in controlling the chemoselectivity of the hydrogenation of fluorinated arenes. Furthermore, the chemical identity of these modifiers and the amount of the silica gel support influence the size distribution of the NPs and thereby the catalytic properties. Finally, we were able to synthesize an active catalyst in a bottom-up approach that has a very similar reactivity compared to the established catalyst. We believe that this approach will enable much more facile means of tuning the catalytic activity of that catalyst system. Hence, the development of next-generation catalysts derived from the studied system is the subject of ongoing research in our laboratories.

■ ASSOCIATED CONTENT

Supporting Information

The Supporting Information is available free of charge at https://pubs.acs.org/doi/10.1021/acscatal.0c01074.

Experimental procedures and spectroscopic and microscopic data (PDF)

■ AUTHOR INFORMATION

Corresponding Author

Frank Glorius − *Organisch-Chemisches Institut, Westfälische Wilhelms-Universität Münster, 48149 Münster, Germany;* orcid.org/0000-0002-0648-956X; Email: glorius@uni-muenster.de

Authors

Daniel Moock − *Organisch-Chemisches Institut, Westfälische Wilhelms-Universität Münster, 48149 Münster, Germany*

Mario P. Wiesenfeldt − *Organisch-Chemisches Institut, Westfälische Wilhelms-Universität Münster, 48149 Münster, Germany;* orcid.org/0000-0002-7142-9336

Matthias Freitag − *Organisch-Chemisches Institut, Westfälische Wilhelms-Universität Münster, 48149 Münster, Germany*

Satoshi Muratsugu − *Department of Chemistry, Graduate School of Science, Nagoya University, Nagoya 464-8602, Aichi, Japan;* orcid.org/0000-0002-3596-7380

Satoru Ikemoto − *Department of Chemistry, Graduate School of Science, Nagoya University, Nagoya 464-8602, Aichi, Japan*

Robert Knitsch − *Institut für Physikalische Chemie, Westfälische Wilhelms-Universität Münster, 48149 Münster, Germany*

Jacob Schneidewind − *Leibniz-Institut für Katalyse e. V., 18059 Rostock, Germany;* orcid.org/0000-0002-5328-6626

Wolfgang Baumann − *Leibniz-Institut für Katalyse e. V., 18059 Rostock, Germany*

Andreas H. Schäfer − *nanoAnalytics GmbH, 48149 Münster, Germany*

Alexander Timmer − *nanoAnalytics GmbH, 48149 Münster, Germany*

Mizuki Tada − *Department of Chemistry, Graduate School of Science and Research Center for Materials Science (RCMS) and Integrated Research Consortium on Chemical Science (IRCCS), Nagoya University, Nagoya 464-8602, Aichi, Japan*

Michael Ryan Hansen − *Institut für Physikalische Chemie, Westfälische Wilhelms-Universität Münster, 48149 Münster, Germany;* orcid.org/0000-0001-7114-8051

Complete contact information is available at: https://pubs.acs.org/10.1021/acscatal.0c01074

Author Contributions

[×]M.P.W. and M.F. contributed equally.

Notes

The authors declare the following competing financial interest(s): The authors declare no conflict of interest. However, please, note that we patented the Process for Synthesizing Fluorinated Cyclic Aliphatic Compounds employing the investigated catalyst system: PCT/EP2018/054554.

■ ACKNOWLEDGMENTS

We are grateful to the European Research Council (ERC Advanced Grant Agreement No. 788558), Fonds der Chemischen Industrie (Kekulé Ph.D. scholarship for D.M. and J.S.), the Studienstiftung des deutschen Volkes (Ph.D. scholarship for M.P.W.), the JST PRESTO Program (No. JPMJPR15S7), the JSPS KAKHENI (Grant No. 18K05144), and Core-to-Core program "Elements Function for Transformative Catalysis and Materials" for generous financial support. TEM and STEM-EDS measurements were conducted at the High Voltage Electron Microscope Laboratory, Institute of Materials and Systems for Sustainability, Nagoya University, supported by "Advanced Characterization Nanotechnology Platform" of MEXT, Japan. XAFS measurements were performed with the approval of PF-PAC (Grant 2017G534) and the Aichi Synchrotron Radiation Center. We are also grateful to C. Schlepphorst, V. Siozios, M. Wollenburg, T. Wagener, A. Heusler, H. Lund, and R. Eckelt for helpful scientific discussions and experimental support.

■ REFERENCES

(1) For an overview on homo- and heterogeneous arene hydrogenation see: (a) Wiesenfeldt, M. P.; Nairoukh, Z.; Dalton, T.; Glorius, F. Selective Arene Hydrogenation for Direct Access to Saturated Carbo- and Heterocycles. *Angew. Chem., Int. Ed.* **2019**, *58*, 10460−10476. (b) *The Handbook of Homogeneous Hydrogenation*; de Vries, J. G., Elsevier, C. J., Eds.; Wiley-VCH: Weinheim, Germany, 2007. (c) *Arene Chemistry: Reaction Mechanisms and Methods for Aromatic Compounds*; Mortier, J., Ed.; John Wiley & Sons, Inc: Hoboken, NJ, 2016. (d) Gual, A.; Godard, C.; Castillón, S.; Claver, C. Soluble Transition-Metal Nanoparticles-Catalysed Hydrogenation of Arenes. *Dalton Trans.* **2010**, *39*, 11499−11512. (e) Qi, S.-C.; Wei, X.-Y.; Zong, Z.-M.; Wang, Y.-K. Application of Supported Metallic Catalysts in Catalytic Hydrogenation of Arenes. *RSC Adv.* **2013**, *3*, 14219−14232. (f) Giustra, Z. X.; Ishibashi, J. S. A.; Liu, S.-Y. Homogeneous Metal Catalysis for Conversion between Aromatic and Saturated Compounds. *Coord. Chem. Rev.* **2016**, *314*, 134−181. (g) Wang, D.-S.; Chen, Q.-A.; Lu, S.-M.; Zhou, Y.-G. Asymmetric Hydrogenation of Heteroarenes and Arenes. *Chem. Rev.* **2012**, *112*, 2557−2590. (h) Zhao, D.; Candish, L.; Paul, D.; Glorius, F. N-Heterocyclic Carbenes in Asymmetric Hydrogenation. *ACS Catal.* **2016**, *6*, 5978−5988.

(2) Lovering, F.; Bikker, J.; Humblet, C. Escape from Flatland: Increasing Saturation as an Approach to Improving Clinical Success. *J. Med. Chem.* **2009**, *52*, 6752−6756.

(3) Previous arene hydrogenation methods from our group employing Rh-CAAC **1**: (a) Wiesenfeldt, M. P.; Nairoukh, Z.; Li,

W.; Glorius, F. Hydrogenation of Fluoroarenes: Direct Access to All-Cis-(Multi)Fluorinated Cycloalkanes. *Science* **2017**, *357*, 908−912. (b) See Tables S9 and S12 for a comparison to a selection of commercial heterogeneous catalysts for the hydrogenation of fluorinated arenes. (c) Wiesenfeldt, M. P.; Knecht, T.; Schlepphorst, C.; Glorius, F. Silylarene Hydrogenation: A Strategic Approach That Enables Direct Access to Versatile Silylated Saturated Carbo- and Heterocycles. *Angew. Chem., Int. Ed.* **2018**, *57*, 8297−8300. (d) Wollenburg, M.; Moock, D.; Glorius, F. Hydrogenation of Borylated Arenes. *Angew. Chem., Int. Ed.* **2019**, *58*, 6549−6553. (e) Arene hydrogenation methods employing Rh-CAACs from other groups: Ling, L.; He, Y.; Zhang, X.; Luo, M.; Zeng, X. Hydrogenation of (Hetero)aryl Boronate Esters with a Cyclic (Alkyl)(amino)-carbene-Rhodium Complex: Direct Access to *cis*-Substituted Borylated Cycloalkanes and Saturated Heterocycles. *Angew. Chem., Int. Ed.* **2019**, *58*, 6554−6558. (f) Zhang, X.; Ling, L.; Luo, M.; Zeng, X. Accessing Difluoromethylated and Trifluoromethylated cis-Cycloalkanes and Saturated Heterocycles: Preferential Hydrogen Addition to the Substitution Sites for Dearomatization. *Angew. Chem., Int. Ed.* **2019**, *58*, 16785−16789. (g) For a lead reference on the chemo- and enantioselective hydrogenation of fluorinated olefins, see Ponra, S.; Rabten, W.; Yang, J.; Wu, H.; Kerdphon, S.; Andersson, P. G. Diastereo- and Enantioselective Synthesis of Fluorine Motifs with Two Contiguous Stereogenic Centers. *J. Am. Chem. Soc.* **2018**, *140*, 13878−13883.

(4) Nairoukh, Z.; Wollenburg, M.; Schlepphorst, C.; Bergander, K.; Glorius, F. The Formation of all-*cis*-(Multi)Fluorinated Piperidines by a Dearomatization−Hydrogenation Process. *Nat. Chem.* **2019**, *11*, 264−270.

(5) Seminal works on the synthesis of CAA(r)Cs by the Bertrand group: (a) Lavallo, V.; Canac, Y.; Präsang, C.; Donnadieu, B.; Bertrand, G. Stable Cyclic (Alkyl)(Amino)Carbenes as Rigid or Flexible, Bulky, Electron-Rich Ligands for Transition-Metal Catalysts: A Quaternary Carbon Atom Makes the Difference. *Angew. Chem., Int. Ed.* **2005**, *44*, 5705−5709. (b) Rao, B.; Tang, H.; Zeng, X.; Liu, L.; Melaimi, M.; Bertrand, G. Cyclic (Amino)(Aryl)Carbenes (CAArCs) as Strong σ-Donating and π-Accepting Ligands for Transition Metals. *Angew. Chem., Int. Ed.* **2015**, *54*, 14915−14919. (c) Reviews: Soleilhavoup, M.; Bertrand, G. Cyclic (Alkyl)(Amino)Carbenes (CAACs): Stable Carbenes on the Rise. *Acc. Chem. Res.* **2015**, *48*, 256−266. (d) Melaimi, M.; Jazzar, R.; Soleilhavoup, M.; Bertrand, G. Cyclic (Alkyl)(Amino)Carbenes (CAACs): Recent Developments. *Angew. Chem., Int. Ed.* **2017**, *56*, 10046−10068.

(6) Lavallo, V.; Canac, Y.; DeHope, A.; Donnadieu, B.; Bertrand, G. A rigid Cyclic (Alkyl)(amino)carbene Ligand Leads to Isolation of Low-Coordinate Transition Metal Complexes. *Angew. Chem., Int. Ed.* **2005**, *44*, 7236−7239.

(7) Wei, Y.; Rao, B.; Cong, X.; Zeng, X. Highly Selective Hydrogenation of Aromatic Ketones and Phenols Enabled by Cyclic (Amino)(Alkyl)Carbene Rhodium Complexes. *J. Am. Chem. Soc.* **2015**, *137*, 9250−9253.

(8) For reviews on the distinction between homo- and heterogeneous catalyst systems see (a) Widegren, J. A.; Finke, R. G. A Review of Soluble Transition-Metal Nanoclusters as Arene Hydrogenation Catalysts. *J. Mol. Catal. A: Chem.* **2003**, *191*, 187−207. (b) Widegren, J. A.; Finke, R. G. A Review of the Problem of Distinguishing True Homogeneous Catalysis from Soluble or Other Metal-Particle Heterogeneous Catalysis under Reducing Conditions. *J. Mol. Catal. A: Chem.* **2003**, *198*, 317−341. (c) Dyson, P. J. Arene Hydrogenation by Homogeneous Catalysts: Fact or Fiction? *Dalton Trans.* **2003**, *15*, 2964−2974 It can be concluded that no singular experiment can unambiguously distinguish between a homo- or heterogeneous nature of the active catalyst and a definitive elucidation requires a series of experiments.

(9) For selected examples of studies on the distinction between a homo- or heterogeneous nature of the active catalyst see (a) Lin, Y.; Finke, R. G. A More General Approach to Distinguishing "Homogeneous" from "Heterogeneous" Catalysis: Discovery of Polyoxoanion- and Bu_4N+-Stabilized, Isolable and Redissolvable, High-Reactivity $Ir_{\sim 190-450}$ Nanocluster Catalysts. *Inorg. Chem.* **1994**, *33*, 4891−4910. (b) Weddle, K. S.; Aiken, J. D.; Finke, R. G. Rh(0) Nanoclusters in Benzene Hydrogenation Catalysis: Kinetic and Mechanistic Evidence That a Putative $[(C_8H_{17})_3NCH_3]$+$[RhCl_4]$-Ion-Pair Catalyst Is Actually a Distribution of Cl- and $[(C_8H_{17})_3NCH_3]$+ Stabilized Rh(0) Nanoclusters. *J. Am. Chem. Soc.* **1998**, *120*, 5653−5666. (c) Bayram, E.; Linehan, J. C.; Fulton, J. L.; Szymczak, N. K.; Finke, R. G. Determination of the Dominant Catalyst Derived from the Classic $[RhCp^*Cl_2]_2$ Precatalyst System: Is It Single-Metal Rh(1)Cp*-Based, Subnanometer Rh_4 Cluster-Based, or $Rh(0)_n$ Nanoparticle-Based Cyclohexene Hydrogenation Catalysis at Room Temperature and Mild Pressures? *ACS Catal.* **2015**, *5*, 3876−3886.

(10) (a) Tran, B. L.; Fulton, J. L.; Linehan, J. C.; Lercher, J. A.; Bullock, R. M. Rh(CAAC)-Catalyzed Arene Hydrogenation: Evidence for Nanocatalysis and Sterically Controlled Site-Selective Hydrogenation. *ACS Catal.* **2018**, *8*, 8441−8449. (b) Tran, B. L.; Fulton, J. L.; Linehan, J. C.; Balasubramanian, M.; Lercher, J. A.; Bullock, R. M. Operando XAFS Studies on Rh(CAAC)-Catalyzed Arene Hydrogenation. *ACS Catal.* **2019**, *9*, 4106−4114.

(11) Chernyshev, V. M.; Astakhov, A. V.; Chikunov, I. E.; Tyurin, R. V.; Eremin, D. B.; Ranny, G. S.; Khrustalev, V. N.; Ananikov, V. P. Pd and Pt Catalyst Poisoning in the Study of Reaction Mechanisms: What Does the Mercury Test Mean for Catalysis? *ACS Catal.* **2019**, *9*, 2984−2995.

(12) For poisoning studies of metals with sulfur-containing compounds see the following book chapter: Bartholomew, C. H.; Agrawal, P. K.; Katzer, J. R. Sulfur Poisoning of Metals. In *Advances in Catalysis*; Eley, D. D., Pines, H., Weisz, P. B., Eds.; Academic Press, 1982; Vol. *31*, pp 135−242;. For a case study see Garbarino, G.; Romero Perez, A.; Finocchio, E.; Busca, G. A Study of the Deactivation of Low Loading Ni/Al2O3 Steam Reforming Catalyst by Tetrahydrothiophene. *Catal. Commun.* **2013**, *38*, 67−73.

(13) Hamlin, J. E.; Hirai, K.; Millan, A.; Maitlis, P. M. A Simple Practical Test for Distinguishing a Heterogeneous Component in a Homogeneously Catalyzed Reaction. *J. Mol. Catal.* **1980**, *7*, 543−544.

(14) Collman, J. P.; Kosydar, K. M.; Bressan, M.; Lamanna, W.; Garrett, T. Polymer-bound Substrates: A Method to Distinguish between Homogeneous and Heterogeneous Catalysis. *J. Am. Chem. Soc.* **1984**, *106*, 2569−2579.

(15) The catalytic system of Rh on SiO_2 can be prepared by stirring **1** with silica gel under hydrogen pressure with or without any substrate. In our studies we have found no difference in reactivity between both cases (see page S23). Different amounts of silica gel can be used, which we have found to have an impact on reactivity. Where appropriate, letters have been used in addition to number **4** in this manuscript to differentiate between catalyst systems prepared under slightly different conditions.

(16) Schwartz, J. Alkane Activation by Oxide-Bound Organorhodium Complexes. *Acc. Chem. Res.* **1985**, *18*, 302−308 Following Schwartz's definition, a heterogeneous catalyst is described by having multiple active sites, as opposed to one active site in a homogeneous catalyst. This definition includes insoluble, supported catalysts, as well as soluble nanoclusters.

(17) An alternative pathway for the amine synthesis is a direct hydrogen splitting starting from the free carbene: Frey, G. D.; Lavallo, V.; Donnadieu, B.; Schoeller, W. W.; Bertrand, G. *Science* **2007**, *316*, 439−441.

(18) For studies analyzing carbenes on surfaces with solid-state NMR techniques, see (a) Baquero, E. A.; Tricard, S.; Flores, J. C.; de Jesús, E.; Chaudret, B. Highly Stable Water-Soluble Platinum Nanoparticles Stabilized by Hydrophilic *N*-Heterocyclic Carbenes. *Angew. Chem., Int. Ed.* **2014**, *53*, 13220−13224. (b) Ernst, J. B.; Muratsugu, S.; Wang, F.; Tada, M.; Glorius, F. Tunable Heterogeneous Catalysis: N-Heterocyclic Carbenes as Ligands for Supported Heterogeneous Ru/K-Al_2O_3 Catalysts to Tune Reactivity and Selectivity. *J. Am. Chem. Soc.* **2016**, *138*, 10718−10721. (c) Ernst, J. B.; Schwermann, C.; Yokota, G.; Tada, M.; Muratsugu, S.; Doltsinis, N. L.; Glorius, F. Molecular Adsorbates Switch on Heterogeneous

https://dx.doi.org/10.1021/acscatal.0c01074
ACS Catal. 2020, 10, 6309−6317

Catalysis: Induction of Reactivity by *N*-Heterocyclic Carbenes. *J. Am. Chem. Soc.* **2017**, *139*, 9144−9147. (d) Baquero, E. A.; Tricard, S.; Coppel, Y.; Flores, J. C.; Chaudret, B.; de Jesús, E. Water-Soluble Platinum Nanoparticles Stabilized by Sulfonated *N*-Heterocyclic Carbenes: Influence of the Synthetic Approach. *Dalton Trans.* **2018**, *47*, 4093−4104.

(19) For recent reviews on the field of carbenes on surfaces, see (a) Hopkinson, M. N.; Richter, C.; Schedler, M.; Glorius, F. An overview of *N*-heterocyclic carbenes. *Nature* **2014**, *510*, 485−596. (b) Zhukhovitskiy, A. V.; MacLeod, M. J.; Johnson, J. A. Carbene Ligands in Surface Chemistry: From Stabilization of Discrete Elemental Allotropes to Modification of Nanoscale and Bulk Substrates. *Chem. Rev.* **2015**, *115*, 11503−11532. (c) Smith, C. A.; Narouz, M. R.; Lummis, P. A.; Singh, I.; Nazemi, A.; Li, C.-H.; Crudden, C. M. *N*-Heterocyclic Carbenes in Materials Chemistry. *Chem. Rev.* **2019**, *119*, 4986−5056. (d) Selected studies: MacLeod, M. J.; Goodman, A. J.; Ye, H.-Z.; Nguyen, H. V.-T.; Van Voorhis, T.; Johnson, J. A. Robust gold nanorods stabilized by bidentate *N*-heterocyclic-carbene-thiolate ligands. *Nat. Chem.* **2019**, *11*, 57−63. (e) Narouz, M. R.; Osten, K. M.; Unsworth, P. J.; Man, R. W. Y.; Salorinne, K.; Takano, S.; Tomihara, R.; Kaappa, S.; Malola, S.; Dinh, C.-T.; Padmos, J. D.; Ayoo, K.; Garrett, P. J.; Nambo, M.; Horton, J. H.; Sargent, E. H.; Hakkinen, H.; Tsukuda, T.; Crudden, C. M. *N*-heterocyclic carbene functionalized magic-number gold nanoclusters. *Nat. Chem.* **2019**, *11*, 419−425.

(20) (a) Astakhov, A. V.; Khazipov, O. V.; Chernenko, A. Yu.; Pasyukov, D. V.; Kashin, A. S.; Gordeev, E. G.; Khrustalev, V. N.; Chernyshev, V. M.; Ananikov, V. P. A New Mode of Operation of Pd-NHC Systems Studied in a Catalytic Mizoroki−Heck Reaction. *Organometallics* **2017**, *36*, 1981−1992. (b) Khazipov, O. V.; Shevchenko, M. A.; Chernenko, A. Yu.; Astakhov, A. V.; Pasyukov, D. V.; Eremin, D. B.; Zubavichus, Y. V.; Khrustalev, V. N.; Chernyshev, V. M.; Ananikov, V. P. Fast and Slow Release of Catalytically Active Species in Metal/NHC Systems Induced by Aliphatic Amines. *Organometallics* **2018**, *37*, 1483−1492.

(21) Kunz, S. Supported, Ligand-Functionalized Nanoparticles: An Attempt to Rationalize the Application and Potential of Ligands in Heterogeneous Catalysis. *Top. Catal.* **2016**, *59*, 1671−1685.

(22) (a) Castelbou, J. L.; Gual, A.; Mercade, E.; Claver, C.; Godard, C. Ligand effect in the Rh-NP catalyzed partial hydrogenation of substituted arenes. *Catal. Sci. Technol.* **2013**, *3*, 2828−2833. (b) Llop Castelbou, J.; Bresó-Femenia, E.; Blondeau, P.; Chaudret, B.; Castillón, S.; Claver, C.; Godard, C. Tuning the Selectivity in the Hydrogenation of Aromatic Ketones Catalyzed by Similar Ruthenium and Rhodium Nanoparticles. *ChemCatChem* **2014**, *6*, 3160−3168. (c) Castelbou, J. L.; Blondeau, P.; Claver, C.; Godard, C. Surface Characterisation of Phosphine and Phosphite Stabilised Rh Nanoparticles: A Model Study. *RSC Adv.* **2015**, *5*, 97036−97043. (d) Foppa, L.; Luza, L.; Gual, A.; Weibel, D. E.; Eberhardt, D.; Teixeira, S. R.; Dupont, J. Sputtering-deposition of Ru nanoparticles onto Al_2O_3 modified with imidazolium ionic liquids: synthesis, characterisation and catalysis. *Dalton Trans.* **2015**, *44*, 2827−2834.

(23) The conditions for the hydrogenation of hexafluorobenzene were chosen to match the optimal conditions for the bottom-up designed system as closely as possible and differ slightly from the best conditions for this system found in our earlier reports (see Table S12 and ref 3c).

https://dx.doi.org/10.1021/acscatal.0c01074
ACS Catal. 2020, 10, 6309−6317